

Dynamical Structures in the Galactic Disk

Alice C. Quillen

Department of Physics and Astronomy, University of Rochester, Rochester, NY 14627, USA
email: aquillen@pas.rochester.edu

Abstract. Resonances with spiral density waves or the Galactic bar can cause structure in local velocity distributions (also known as phase space). Because resonances are narrow, it is possible to place tight constraints on a pattern speed or the shape of the underlying gravitational potential.

Interference between multiple spiral patterns can cause localized bursts of star formation and discontinuities or kinks in the spiral arm morphology. Numerical simulations suggest that boundaries between different dominant patterns in the disk can manifest in local velocity distributions as gaps that are associated with specific orbital periods or angular momentum values. Recent studies have detected age gradients that may be associated with the appearance of spiral features such as armlets and spurs.

When patterns grow or vary in speed, resonances can be swept through the disk causing changes in the velocity distributions. Evidence of resonance capture or resonance crossing can be used to place constraints on the past history of patterns in the disk. The X-shaped Galactic bulge may have been caused by stars captured into vertical resonance with the Bar.

Disturbances in the Galactic disk, such as from a past merger, can cause an uneven distribution of disk stars in action angles. Subsequently the stellar distribution becomes more tightly wound in phase space. Phase wrapping can cause a series of shell like features in either real space or in a local velocity distribution. The spacing between features is dependent on the time since the disturbance.

Keywords. Galaxy: disk, Galaxy: kinematics and dynamics, (Galaxy:) solar neighborhood, Galaxy: structure

1. Introduction

Hipparcos observations (Dehnen & Binney 1998) confirmed Eggen's hypothesis (Eggen 1996) that the stellar velocity distribution in the Solar neighborhood is not smooth, but contains a wealth of dynamical structure that we refer to as streams and moving groups. Forthcoming large scale Galactic surveys, including LAMOST and Gaia, will reveal increasing levels of detail and will show how these kinematic structures vary as a function of position in the Galaxy. This is an exciting time for dynamicists as this structure can be used to make precise measurements, reveal the current structure of the Galaxy disk, and unravel its past history. In this review I will focus on how dynamical structures in the Galactic disk are induced by bar, spiral patterns and external perturbations.

2. Interpreting structure in the uv plane

To understand structure in local velocity distributions it is helpful to recall properties of stellar orbits. In the absence of perturbations from spiral arms or bar, the motion of stars in the disk of a galaxy can be described in terms of radial or epicyclic oscillations about a circular orbit. The radial and tangential velocity components, u, v , are related to the parameters describing the epicyclic motion; the mean radius or guiding radius, r_g ,

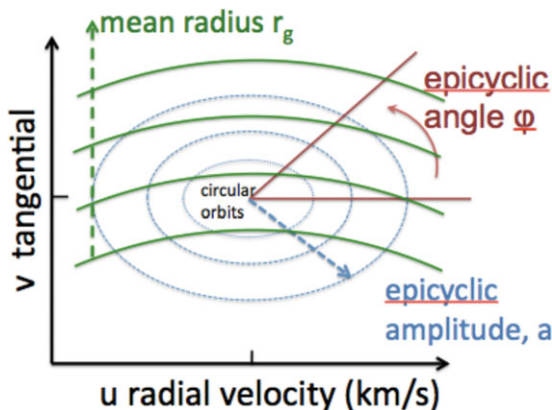


Figure 1. The relation between position in the uv plane and orbital properties. The x and y axes are the radial, (u), and tangential velocity, (v), components for the distribution of stars in the Solar neighborhood. Stars with high v have high angular momentum and so have guiding (or mean) radii outside the Solar neighborhood. Stars with low v have lower angular momentum and so have mean radii inside the Solar radius. The orbital period is dependent on v , so resonances with patterns are encountered at different v values.

and the epicyclic amplitude, a . The energy of an orbit in the plane of an axisymmetric system (neglecting perturbations from spiral arms or bar) with a flat rotation curve is

$$E(u, v) = \frac{(v_c + v)^2}{2} + \frac{u^2}{2} + v_c^2 \ln r + \text{constant} \tag{2.1}$$

where the potential energy, $\propto \ln r$, is that appropriate for a flat rotation curve, r is the galactocentric radius and v_c is the circular velocity.

With an epicyclic approximation we can write the energy

$$E = v_c^2 \left[\frac{1}{2} + \ln r_g \right] + E_{epi} \tag{2.2}$$

where the term on the left is the energy of a star in a circular orbit about a guiding radius r_g and E_{epi} is the energy from the epicyclic motion,

$$E_{epi} = \frac{u^2}{2} + \frac{\kappa^2 (r - r_g)^2}{2} = \frac{\kappa^2 a^2}{2}. \tag{2.3}$$

Here a is the epicyclic amplitude and κ is the epicyclic frequency at the guiding radius, r_g .

We now consider stars specifically in a neighborhood of galactocentric radius r_0 , restricting us to a specific location in the galaxy. Setting the energy equal to that written in terms of the epicyclic motion using equations (2.2, 2.3), we solve for the guiding radius, r_g . It is convenient to define the distance between the guiding or mean radius and the neighborhood’s galactocentric radius, $s = r_g - r_0$. To first order in v and s we find that a star in the neighborhood with velocity components u, v has a guiding radius with and epicyclic amplitude

$$\frac{s}{r_0} \approx \frac{v}{v_c}, \quad \frac{a}{r_0} \approx v_c^{-1} \sqrt{\frac{u^2}{2} + v^2}. \tag{2.4}$$

The factor of a half is from κ^2/Ω^2 equivalent to 2 when the rotation curve is flat. An

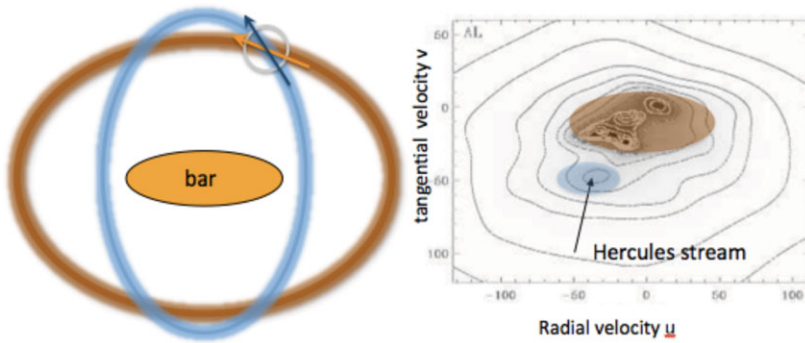


Figure 2. At a particular v velocity component value the outer Lindblad resonance with the Galactic Bar is crossed. Orbits in the Solar neighborhood (shown on the left) are divided into two families, those that are aligned with the Bar and those that are perpendicular to the bar. Positions on the uv plane correspond to orbit orientations. As there are few stellar orbits with intermediate vectors, there is a gap in the velocity distribution shown on the right. On the right we show the Solar neighborhood velocity distribution by Dehnen & Binney (1998) with colors overlaid to show the two families of orbits that are shown on the left.

angle describing the phase in the epicycle is

$$\phi \sim \text{atan} \left(\frac{-u}{\sqrt{2}v} \right). \quad (2.5)$$

The epicyclic phase angle $\phi = 0$ at apocenter.

The above three relations let us relate the velocity components (u, v) for stars in the Solar neighborhood, to quantities used to describe the epicyclic motion; the guiding radius, epicyclic amplitude and epicyclic phase angle. This relationship is illustrated in Figure 1.

2.1. Lindblad Resonances and their Connection to The Kirkwood Gaps

The rotation or orbital period of a star is primarily set by the guiding radius r_g and in a particular local neighborhood, this is approximately set by the v velocity component or equivalently, the star's angular momentum. The v velocity component can be considered an analogous to the semi-major axis in celestial mechanics because it determines the orbital period. For example, the spatial distribution of asteroids on the ecliptic plane contains little structure. Only when the distribution is plotted as a function of semi-major axis are the Kirkwood gaps seen in the asteroid distribution. The Kirkwood gaps are dips in the number of asteroids at particular semi-major axis values. These are orbital resonances with Jupiter and occur where

$$jn \approx kn_J \quad (2.6)$$

for n and n_J the mean motions (approximately angular rotation rate) of asteroid and Jupiter, respectively and j, k are integers. Orbital resonances are seen in the semi-major axis distribution because the orbital periods depend on the semi-major axis. Orbital resonances can be seen in the v distribution in the Solar neighborhood because v sets the orbital period.

The largest feature in the Solar neighborhood's velocity distribution is a gap separating nearly circular orbits with the Hercules stream at $(u, v) \approx (-50, -50) \text{ km s}^{-1}$. The gap is likely due to the outer Lindblad resonance with the Galactic bar (e.g., Dehnen 2000).

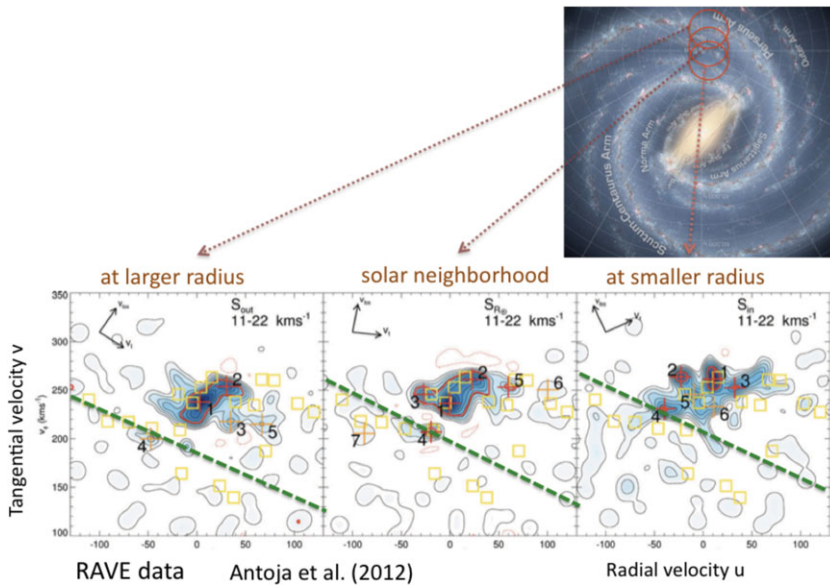


Figure 3. The v velocity component value of the Bar's outer Lindblad resonance depends on a neighborhood's galactocentric radius. Hence the location of the gap in the velocity distribution shifts as a function of the neighborhood's galactocentric radius. Shown here is a figure by Antoja *et al.* (2012) illustrating that the gap in the RAVE survey velocity distribution, separating the Hercules stream, is a function of neighborhood location in the Galaxy.

This resonance obeys a commensurability

$$\kappa + 2(\Omega - \Omega_b) \sim 0 \quad (2.7)$$

similar in form to equation 2.6 for resonances in the asteroid belt. On resonance there are no circular orbits. Low eccentricity orbits are either aligned with or perpendicular to the bar and so are separated into two families. In a local region, these two families have different orientation vectors. The stellar distribution is divided into two clumps, orbits aligned with the bar and those aligned perpendicular to the bar. Each position on the uv plane corresponds to a different orbit orientation. Stars in the Hercules stream correspond to orbits oriented perpendicular to the bar and those near the origin are oriented parallel to the bar. The gap corresponds to the absence of intermediate orientation orbits exactly in resonance. This is illustrated in Figure 2.

2.2. Resonances Allow Precise Measurements

Because the ratio of the bar gravitational potential perturbation strength to the axisymmetric value is small (less than a percent), the outer Lindblad resonance is not a wide resonance. As a consequence, the bar pattern speed has been very precisely measured. For example Gardner & Flynn (2010a,b), measure $\Omega_b/\Omega_\odot = 1.87 \pm 0.02$, consistent with that by Minchev *et al.* (2007). Here Ω_\odot is the angular rotation rate of a star in a circular orbit with the Sun's galactocentric radius and neglecting perturbations from spiral or bar perturbations. Similar levels of precision arise when gaps at lower u, v are modeled with resonances associated with spiral patterns (Quillen & Minchev 2005, Lepine *et al.* 2011). These studies explored the role of the 4:1 Lindblad resonance with a spiral pattern showing that diamond shaped orbits were present on one side and square shaped orbits on the opposite side of resonance.

2.3. Locations of Resonances in local velocity distributions from different neighborhoods

A prediction of the resonant model for the Hercules stream is that the location of the gap should depend on location in the Galaxy. We consider the location of the gap for neighborhoods with galactocentric radii that are larger or smaller than that of the Sun (at galactocentric radius R_{\odot}). We would expect that a neighborhood with galactocentric radius inside R_{\odot} , is closer to the outer Lindblad resonance and so the gap in the velocity distribution would be at a v value closer to 0. Likewise a neighborhood at a larger galactocentric radius than R_{\odot} is more distant from the resonance, and the velocity distribution should have a gap at a more negative v value. Recent observations allow velocity distributions to be constructed at more distant regions from the Sun than previously possible using Hipparcos observations. A very exciting recent discovery is this that a shift in gap v value has been detected using RAVE survey observations Antoja *et al.* (2012). The shift in the gap velocity as a function of neighborhood galactocentric radius is illustrated using a Figure by Antoja *et al.* in Figure 3.

3. Local Velocity Distributions in an N-body simulation

Forthcoming large scale surveys, such as LAMOST and Gaia, will probe deeper into the Galaxy than Hipparcos and RAVE surveys and so will allow us to look at velocity distributions in more distant regions of the Galaxy. In preparation for these surveys we can examine local velocity distributions in an N-body simulation. With recent advances in computational hardware and software, it is now possible to run simulations with sufficient numbers of particles that velocity distributions can be extracted from small regions in a simulated galaxy disk. The simulation we discuss is that described by Quillen *et al.* (2011) with initial conditions chosen so that the simulated galaxy is similar to the Milky Way (using the prescription by Widrow *et al.* 2008). The halo is live. Massless tracer particles are simultaneously integrated along with the massive particles. The number of test (massless) particles in the disk is 3 million and exceeds the number of simulated massive disk particles by a factor of 3.

In this section we discuss the properties of velocity distributions extracted from circular regions (neighborhoods) centered at different azimuthal angles and galactocentric radii (see Figure 4). Each neighborhood has radius 0.1 times that of its galactocentric radius. Velocity distributions extracted from the positions shown in Figure 4 are shown in Figure 5. The local velocity distributions exhibit gaps, arcs, and clumps *everywhere* in the galaxy disk. Higher velocity dispersions are found on spiral arm peaks.

Gaps seen in the distributions from bordering neighborhoods tend to be at shifted v velocity, suggesting that they are associated with particular rotational periods. Rather than being clearly associated with Lindblad resonances, we suspect that gaps in the velocity distribution are associated with transitions between different spiral patterns. We tended to see gaps when and where there were discontinuities in the spiral arms such as changes in angle or kinks. The cartoon shown in Figure 6 illustrates why a discontinuity in spiral structure might account for a gap in a local velocity distribution.

3.1. A location in the simulation like the Solar neighborhood

We chose positions in our N-body simulation near the position of the bar's outer Lindblad resonance and with bar orientation similar to that expected for the solar neighborhood. When there was a strong spiral arm, just interior to this mock solar neighborhood, and consistent with the Centaurus arm, then the velocity distribution is similar to that seen in the Solar neighborhood. Three such times and positions are shown in Figure 7. The morphology of these three snapshots is similar near the mock solar neighborhood,

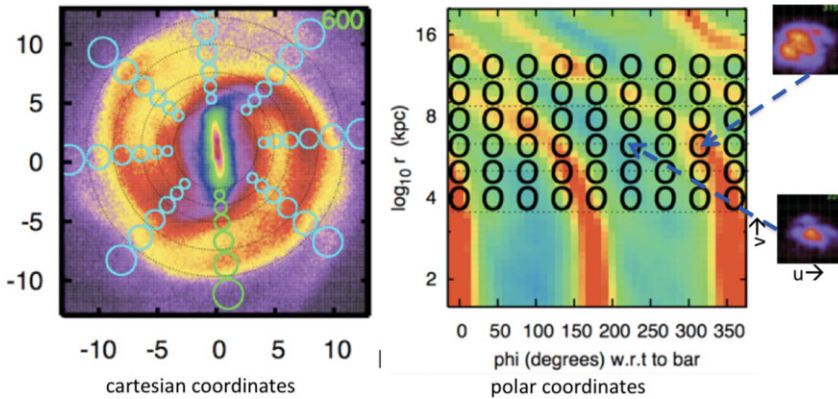


Figure 4. Here we show the surface density of a single snapshot in an N-body simulation. On the left is the disk surface density in Cartesian coordinates. On the right the differential disk surface density is shown as a function of the log of the radius r and azimuthal angle. A logarithmic spiral arm has high densities along a line on this plot with pitch angle given by the slope of the line. Overlain on these plots are neighborhoods where we have extracted local velocity distributions. Interarm velocity distributions (as shown on the top right) are more compact than those taken from spiral arm peaks. In the rightmost panel, the patterns move to the right with time and trailing structures have negative slopes. Exterior to the bar, both two-armed and three-armed patterns are seen and their patterns move more slowly than the bar. On an animated version of this panel it is clear that patterns in the inner galaxy are faster than those in the outer galaxy. Interference between the patterns sometimes causes armlets to appear and disappear. See Quillen *et al.* (2011) for more information.

however the morphologies of the opposite side of the galaxy are quite different. The Solar neighborhood velocity distribution alone is not sufficient to break the degeneracies of a model that includes multiple spiral waves. More importantly, all three of these snapshot images show strong three-arm structure. Models of our galaxy are often bi-symmetric (only containing two- and four-armed patterns). However, if the Galactic bar couples to a lopsided or $m = 1$ motion, then our Galaxy may contain a strong three-armed pattern in the vicinity of the Solar neighborhood.

3.2. Star formation gradients and Interference between spiral patterns

Often assumed is that spiral arms advance in a steady fashion across a galaxy disk. However if multiple patterns are present, spiral features may appear and then disappear due to interference between patterns. This would cause localized bursts of star formation rather than a steady wave of star formation crossing the galactic disk. A local burst of star formation would manifest as a gradient in the age distribution of young stars. Through spectroscopic studies it may be possible to find such progressions of star formation in the Galaxy. A particularly exiting recent discovery is the age gradient in the Sco-Cen moving group (Pecaut, Mamajek & Bubar 2012, Pecaut 2013). The age gradient (see Figure 8a) corresponds to about 10 Myr across a region of 100 pc. This corresponds to a slow speed of only 10 km/s. This burst of star formation may be due to a small armlet that appeared interior to the Solar neighborhood about 20 Myr ago, or it may be a spur from a larger nearby spiral feature such as the Centaurus arm.

Ultraviolet imaging has recently revealed age gradients in nearby disk galaxies (Sanchez-Gil *et al.* (2011)). A figure from this work is shown as Figure 8b. The red circle on this plot points out a region where the age gradient is approximately 5 Myr across a region a few kpc in length. This corresponds to a velocity of about 500 km/s, exceeding the

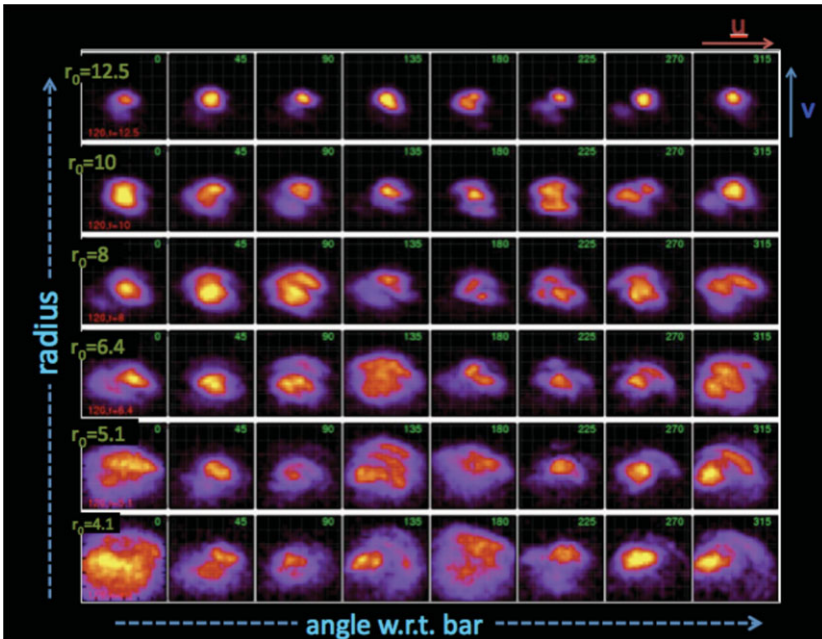


Figure 5. Local velocity distributions extracted at the positions shown in Figure 4 from an N-body simulation snapshot. The local velocity distributions exhibit gaps, arcs, and clumps *everywhere* in the galaxy disk. Higher velocity dispersions are found on spiral arm peaks. Gaps seen in the distributions from bordering neighborhoods tend to be at shifted v velocity, suggesting that they are associated with particular rotational periods. These gaps are likely associated with resonances or transitions between spiral patterns.

galactic circular velocity! This suggests that the large age gradient cannot be due to a single spiral pattern and so could be due to the appearance of a short lived feature.

These two studies (Pecaut 2013, Sanchez-Gil *et al.* 2011), are very exciting as they suggest that deeper and more detailed studies may reveal time dependent distributions of star formation. Perhaps it will be possible to differentiate between models of spiral structure and understand how star formation is triggered. See Claire Dobb's paper in this volume and Dobbs & Pringle (2010) for more exploration on patterns of star formation.

4. Phase Wrapping

Within the context of a Hamiltonian model, a system is said to be in action angle variables if the Hamiltonian of the system can be written in terms of actions alone. Then because of Hamilton's equations, the actions (momenta) are conserved. A dynamically relaxed system can be described in terms of a distribution in action variables alone. This is equivalent to assuming that the system is evenly distributed in the angles.

However, a distribution of stars that is initially not evenly distributed in action angle would exhibit structure in both real space and velocity space as the distribution in phase space is projected to a lower dimension. This is illustrated in Figure 9. Most studies have focused on how a disrupted dwarf galaxy, originally localized in phase space, would be seen as a stellar stream. However a disturbance in the Galactic *disk*, such as caused by a merger, would also cause an uneven distribution in action angle. This can cause shell-like structures (Minchev *et al.* 2009) or clumps (Quillen *et al.* 2009) in local velocity distributions. Such phenomena has also recently been seen in N-body simulations (Gomez

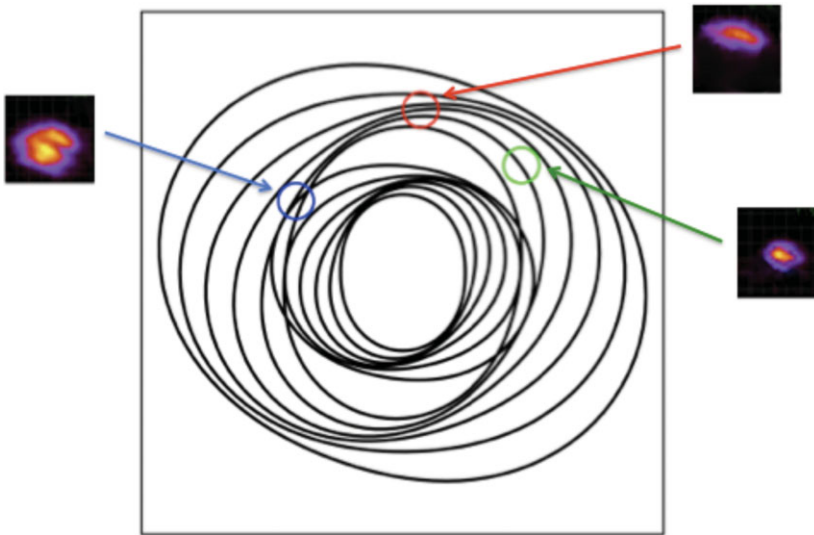


Figure 6. How spiral structure affects local velocity distributions. The red circle is an example of an arm peak. There are a large range of velocities or orbit orientations in a region where many elliptical orbits overlap, giving an arc in the velocity distribution. In interarm regions, (e.g., green circle) the range of velocities (or angles on this plot) in a particular neighborhood is low and so the corresponding velocity dispersion in this neighborhood is also low. The blue circle is located at a radius where there is a discontinuity in spiral structure and shows that the angular distribution of orbits is bifurcated. We expect that in such a region there will be gap in the velocity distribution.

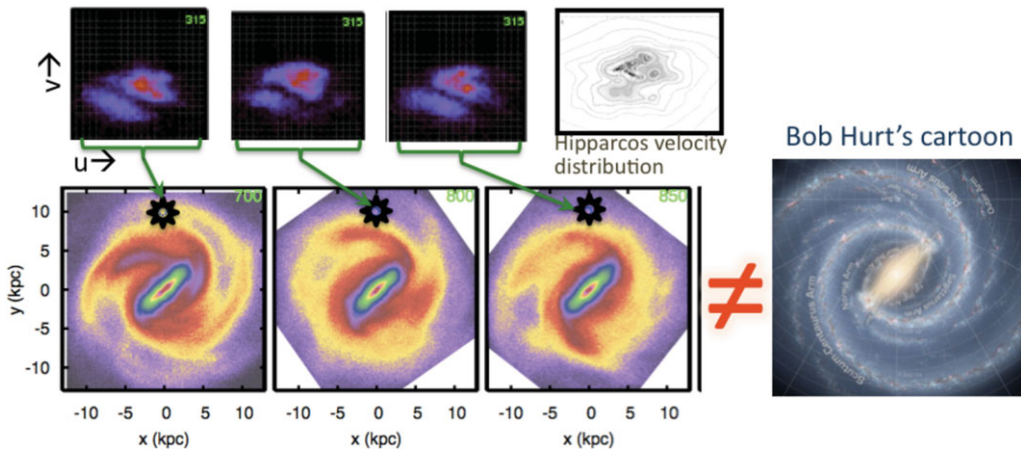


Figure 7. Velocity distributions resembling that in the Solar neighborhood are shown from three different simulation snapshots. The locations are chosen to lie just outside the bar's outer Lindblad resonance and with bar orientation appropriate for the Solar neighborhood. The velocity distributions resemble that seen in the Solar neighborhood when there is a strong spiral arm just interior to the Sun, similar to the Centaurus arm. Models are poorly constrained on the opposite side of the Galaxy. Models of our galaxy, such as shown in the right, display bi-symmetry (only containing two and four armed patterns). If the Galactic Bar ($m = 2$) couples to a lopsided or $m = 1$ motion, then our Galaxy may contain a strong three-armed pattern in the vicinity of the Solar neighborhood.

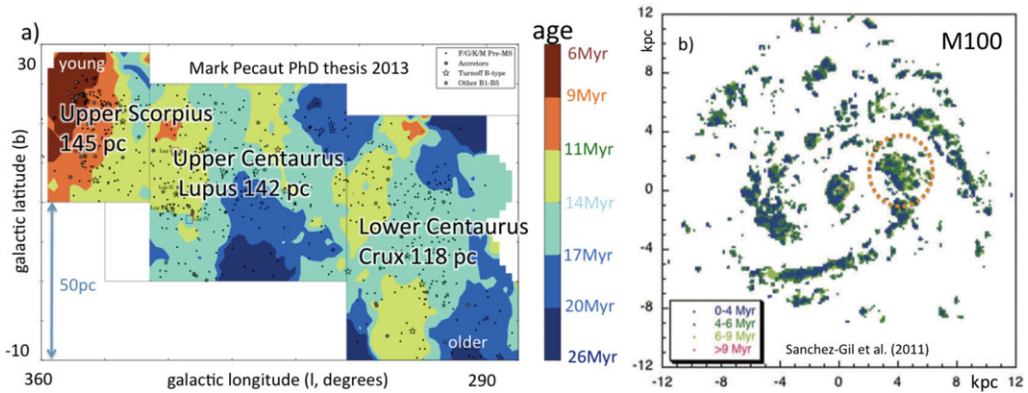


Figure 8. Recent discoveries of age gradients. a) An age gradient of 10 Myr across 150 pc has recently been discovered in the distribution of stars in the Sco-Cen moving group (Pecaut, Mamajek & Bubar 2012). This figure is from Pecaut (2013). b) Using UV imaging, age gradients have been detected in nearby galaxies such as M100 and shown on the right; figure by Sanchez-Gil *et al.* (2012). The red circle points out a region with age gradient and a velocity so high that it exceeds the galactic circular velocity and so is more likely due to the recent appearance of a spiral feature than the advance of a single pattern.

et al. 2012). The separation between shells gives a constraint on the timescale since the perturbation.

5. Resonance Capture Model for the X-shaped Bulge

An exciting recent discovery is that the Galactic bulge, as traced by red-clump giants, displays a bimodal brightness distribution (Nataf *et al.* 2010, McWilliam & Zoccali 2010). The observed distributions can be explained with a vertical X-shaped structure in the bulge region (Li & Shen 2012). Numerous numerical studies have explored the growth of peanut or X-shaped bulges in response to bar buckling. Here instead I focus on the resonance capture interpretation (Quillen 2002) which is not inconsistent with either bar buckling (Raha *et al.* 1991) or the association of the X-shape with banana shaped orbits (Pfenniger & Friedli 1991, Patsis *et al.* 2002). The resonance capture model for the formation of a peanut has an analogy in celestial mechanics. As Neptune migrates outwards, Pluto is captured into resonance with Neptune. As Neptune continues to migrate outwards, Pluto’s eccentricity increases. As the bar grows or slows down, stars are captured into the vertical resonance with the bar. As the bar continues to grow or continues to slow down, particles are lifted in inclination.

A vertical Lindblad resonance is a commensurability where there are two vertical oscillations per rotation in the frame moving with the bar;

$$\nu \approx 2(\Omega - \Omega_b) \tag{5.1}$$

where ν is the vertical oscillation frequency, Ω the angular rotation rate of a star in a circular orbit and Ω_b the bar pattern speed. Integrating the above relation we find an angle

$$\phi \equiv \theta_3 - 2(\theta - \Omega_b t) \sim \text{constant} \tag{5.2}$$

where θ_3 is the action angle associated with vertical oscillations, and θ is the azimuthal angle in the galaxy mid-plane. The above resonant angle is fixed for banana shaped

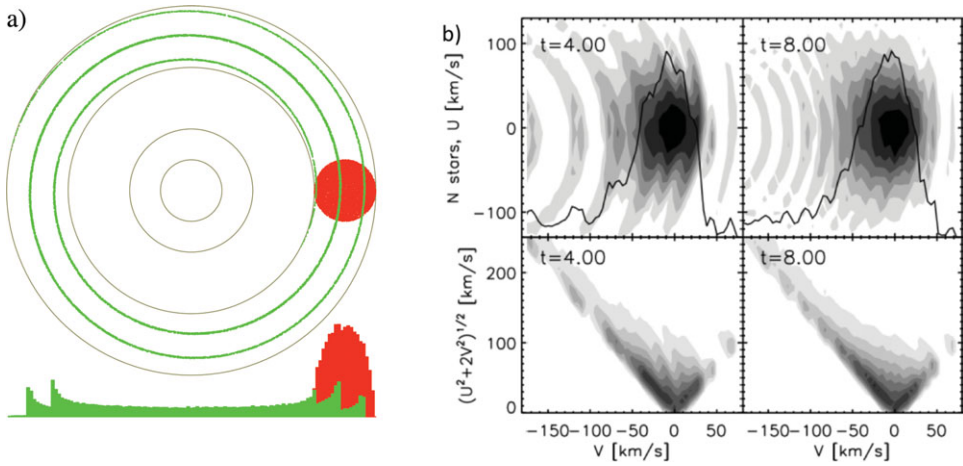


Figure 9. Phase wrapping in the Galactic disk. a) A group of stars, initially in a small compact region of phase space and shown in red, evolves in action angle as a function of time. Later on the same group of stars, shown in green, is widely distributed in action angle and sheered into a narrow spiral in phase space. On the top plot, the radius from the origin corresponds to an action variable. Or equivalently, when epicyclic oscillations are considered, the x axis could correspond to radial velocity and the y axis to galactocentric radius. Black circles show orbits with constant action variable. When projected into either real space or velocity space, the distribution (shown on the bottom) contains structure at the later time. Shells become narrower and closer together as a function of time. A perturbation to the Galactic disk (such as from a merger) can cause an uneven distribution in action angle. At later times, shells can be seen in local velocity distributions and their separation can give constraints on the time since the perturbation. b) Shells seen a local velocity distribution from a simulation of a perturbed thick disk. The left panels are at an earlier time than the right panels. The distance between shells is a function of time. This figure is by Minchev *et al.* (2009).

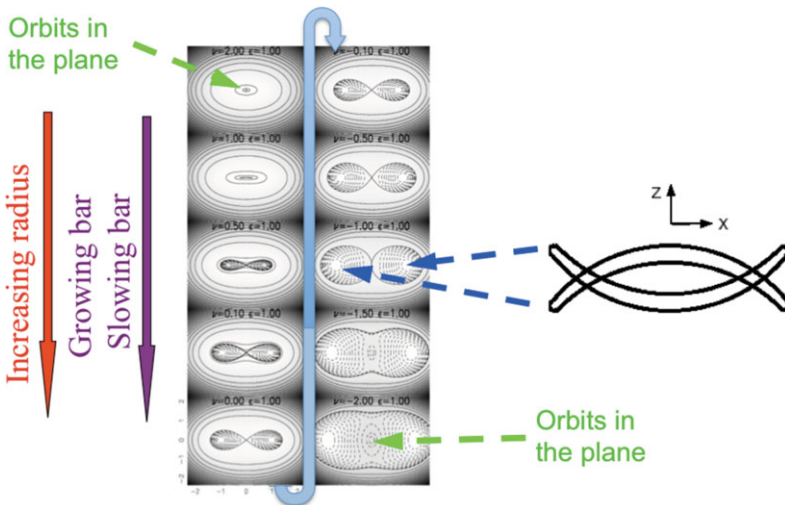


Figure 10. A Hamiltonian model for a vertical Lindblad resonance. Level curves of the Hamiltonian (equation 5.3) are shown as a function of distance from resonance or bar strength. As the bar slows down or grows, stars originally at low inclination can be lifted into high inclination orbits. In this case stars in the peanut or X-shape part of the bulge have been captured into the vertical resonance with the bar.

periodic orbits. The action momentum conjugate to θ_3 we call J and this scales with orbital inclination or vertical oscillation amplitude.

A Hamiltonian model can be constructed in the vicinity of the vertical resonance

$$H(J, \phi) = aJ^2 + \delta J + \epsilon J \cos 2\phi \quad (5.3)$$

where the first two terms depend solely on the unperturbed galaxy potential, or that lacking the Galactic bar. Here a depends on the derivatives of the gravitational potential with respect to z . The coefficient $\delta = \nu/2 - (\Omega - \Omega_b)$ determines the distance to resonance, with $\delta \sim 0$ on resonance. The rightmost term is due to the bar perturbation. The coefficients a, δ, ϵ are dependent on radius. Level contours of this Hamiltonian are shown in Figure 10. The level curves of the Hamiltonian depend both on the distance to resonance, δ , and the bar perturbation strength, ϵ . As the bar grows, ϵ increases. As the bar slows down δ would decrease. Both variations cause the Hamiltonian level curves to go downwards on this Figure. Stars originally in the mid plane can be lifted into high inclination orbits. Stars in the peanut or X-shape part of the bulge can be described as captured into the vertical resonance with the bar. Such a model has not yet been applied to the Milky Way's bulge. However, this model, if successful, may place constraints not only on the current shape of the bulge, but on how the bar grew.

References

- Antoja, T., *et al.* 2012, *MNRAS*, 426, L1
 Dehnen, W. & Binney, J. J. 1998, *MNRAS*, 298, 387
 Dehnen W. 2000, *AJ*, 119, 800
 Dobbs, C. L. & Pringle, J. E. 2010, *MNRAS*, 409, 396
 Eggen, O. J. 1996, *AJ*, 112, 1595
 Gardner, E. & Flynn, C. 2010, *MNRAS*, 405, 545
 Gardner, E. & Flynn, C. 2010, *MNRAS*, 406, 701
 Gómez, F. A., Minchev, I.; Villalobos, A., O'Shea, B. W., & Williams, M. E. K. 2012, *MNRAS*, 419, 2163
 Lépine, J. R. D., Roman-Lopes, A., Abraham, Zulema, Junqueira, T. C., & Mishurov, Yu. N. 2011, *MNRAS*, 414, 1607
 Li, Z.-Y. & Shen, J. 2012, *ApJ*, 757, L7
 McWilliam, A. & Zoccali, M. 2010, *ApJ*, 724, 1491
 Minchev, I., Nordhaus, J., & Quillen, A. C. 2007, *ApJ*, 664, L31
 Minchev, I., Quillen, A. C., Williams, M., Freeman, K. C., Nordhaus, J., Siebert, A., & Bienaymé, O. 2009, *MNRAS*, 396, 56
 Nataf, D. M., Udalski, A., Gould, A. Fouque, P., & Stanek, K. Z. 2010, *ApJ*, 721, L28
 Pecaute, M. J., Mamajek, E. E., & Bubar, E. J. 2012, *ApJ*, 746, 154
 Pecaute, M. J. 2013, PhD thesis, University of Rochester
 Pfenniger, D., & Friedli, D. 1991, *A&A*, 252, 75
 Quillen, A. C. 2002, *AJ*, 124, 722
 Quillen, A. C. 2003, *AJ*, 125, 785
 Quillen, A. C., & Minchev, I. 2005, *AJ*, 130, 576
 Quillen, A. C., Minchev, I., Bland-Hawthorn, J., & Haywood, M. 2009, *MNRAS*, 397, 1599
 Quillen, A. C., Dougherty, J., Bagley, M. B.; Minchev, I., & Comparetta, J. 2011, *MNRAS*, 417, 762
 Patsis, P. A., Skokos, C., & Athanassoula, E. 2002, *MNRAS*, 337, 578
 Raha, N., Sellwood, J. A., James, R. A., & Kahn, F. D. 1991, *Nature*, 352, 411
 Sánchez-Gil, M. C., Jones, D. H., Pérez, E., Bland-Hawthorn, J., Alfaro, E. J., & OByrne, J. 2011, *MNRAS*, 415, 753
 Widrow, L. M., Pym, B., & Dubinski, J. 2008, *ApJ*, 679, 1239

Discussion

GIACOMO MONARI: In your N-body simulation you have selected regions that have kinematics similar to the Solar neighborhood. Is the gap in the velocity distribution (separating the Hercules stream) due to the Bar or discontinuities associated with spiral arms?

ALICE QUILLEN: In the Solar neighborhood, perturbations due to spiral structure are stronger than that associated with the Bar, however there may not be a nearby strong resonance with a spiral pattern. So far, only models with a Galactic bar have successfully accounted for the gap in the velocity distribution separating the Hercules stream from the rest of the stars in the Solar neighborhood's velocity distribution. In our N-body simulations, a strong gap in the local velocity distribution was only seen when there was a strong spiral arm just interior to the position of the Solar neighborhood. At other times, local spiral structure can obscure the signature of the Bar's outer Lindblad resonance and there was no strong gap (or no gap at the appropriate v value). Our simulation does show gaps that are not associated with Lindblad resonances with the Bar, so it is possible that the gap separating the Hercules stream, in the Solar neighborhood's velocity distribution, has been misinterpreted with bar models. Spiral waves could be driven at the bar's outer Lindblad resonance so a gap may be present in the velocity distribution if there is coupling between bar and spiral patterns. In this case the gap could be associated with the Bar's outer Lindblad resonance, a resonance of a spiral density wave *and* a transition between two different pattern spiral waves.

YANG HUANG: You mentioned work by Eric Mamajek and Marc Picaud measuring an age gradient in the Sco/Cen moving group. How were the ages measured? Other studies have not found an age gradient.

ALICE QUILLEN: X-ray and proper motion surveys were used to improve the census of stars in all three subgroups of the Sco-Cen association. Spectroscopic observations of nearby, young moving groups were used to construct an improved spectral type intrinsic color T_{eff} /bolometric correction. The mean ages of each subgroup were estimated from the high-mass main sequence turn-off stars, and the location of both F-type and G-type moving group members on the HR diagram. Please see Picaud *et al.* (2012) and Mark Picaud's PhD thesis (2013). I urge you to contact Eric Mamajek and Marc Picaud for more information about their study.

TERESA ANTOJA: I find the complexity of the numerically simulated local velocity distributions daunting. If the Galaxy displays such complexity it may be very difficult to model and understand.

ALICE QUILLEN: I agree. Perhaps our Galaxy is less complex than the simulation I showed? The complexity of the dynamics is a good motivation to better understand spiral structure. The prospect that we will be able to not only better understand the current structure of the Milky Way but its evolution is very exciting, but it may take some thought and effort to create predictive and illuminating models.